Reduction of Topological Z Classification in Cold-Atom Systems

Tsuneya Yoshida, Ippei Danshita, Robert Peters, and Norio Kawakami

Phys. Rev. Lett. **121**, 025301 — Published 9 July 2018

DOI: 10.1103/PhysRevLett.121.025301

Reduction of topological $\mathbb{Z}$ classification in cold atomic systems

Tsuneya Yoshida,[1] Ippei Danshita,[2] Robert Peters,[1] and Norio Kawakami[1]

[1] *Department of Physics, Kyoto University, Kyoto 606-8502, Japan*

[2] *Yukawa Institute for Theoretical Physics, Kyoto University, Kyoto 606-8502, Japan*

(Dated: May 1, 2018)

One of the most challenging problems in correlated topological systems is a realization of the reduction of topological classification, but very few experimental platforms have been proposed so far. We here demonstrate that ultracold dipolar fermions (e.g., ^{167}Er, ^{161}Dy, and ^{53}Cr) loaded in an optical lattice of two-leg ladder geometry can be the first promising testbed for the reduction $\mathbb{Z} \to \mathbb{Z}_4$, where solid evidence for the reduction is available thanks to their high controllability. We further give a detailed account of how to experimentally access this phenomenon; around the edges, the destruction of one-particle gapless excitations can be observed by the local radio frequency spectroscopy, while that of gapless spin excitations can be observed by a time-dependent spin expectation value of a superposed state of the ground state and the first excited state. We clarify that even when the reduction occurs, a gapless edge mode is recovered around a dislocation, which can be another piece of evidence for the reduction.

Introduction.- After the discovery of topological insulators, a topological perspective on condensed matter physics has become increasingly important[1,2]. The notion of topological phases has been extended to topological semi-metals and topological superconductors. Remarkably, these phases host exotic particles as low energy excitations, such as Weyl fermions, Majorana fermions *etc.*, some of which have potential applications to quantum computations[3,4].

The discovery of topological insulators has further brought great impact beyond solid state physics. In particular, it has provided a new arena of study in cold atoms, which is rapidly developing in these years[5–8]. A significant advantage of cold atoms over materials is the high controllability, which has allowed unique observations for non-interacting topological systems, such as the Zak phase[5], the Thouless pump[7,8], and a symmetry-protected topological state[9]. With this remarkable success, it is not hard to imagine that the high controllability would be a key for solving one of the most significant issues in topological condensed matter physics, i.e. correlation effects on topological insulators/superconductors. Therefore, combining topology and strong correlations in cold atoms would provide a new perspective on correlated topological systems.

One of the striking phenomena induced by correlations in topological systems is the reduction of topological classification. Namely, correlation effects reduce the number of possible topological phases under certain symmetry classes. For instance, topological superconductors of symmetry class BDI follow $\mathbb{Z}$ classification in the absence of correlations while the systems follow $\mathbb{Z}_8$ classification in the presence of correlations[10]. In other words, eight Majorana fermions arising from the winding number $\nu = 8$ are completely gapped out without symmetry breaking or gap-closing in the bulk. Extensive studies on this issue[11–29] have revealed that the reduction occurs in any dimension and is ubiquitous.

In spite of the above remarkable discovery, the following crucial question remains unsolved: *How can one realize a testbed to observe the reduction of topological classification?* The experimental observation is indispensable for further developments in correlated topological systems, and therefore such a feasible platform to observe the reduction is highly desired. For solid evidence of the reduction, tuning the interaction is considered to be a key technique, but is rather difficult to control in the platform for solids[29]. If one could find how to prepare such a platform, it would bring significant progress toward the observation of the reduction. Unfortunately, however, very few experimental platforms have been proposed so far.

With this background, we tackle the above problem by focusing on cold atoms, in which system's parameters can be widely controlled. As a first step toward detection of the reduction, we here consider the simplest case, a one-dimensional correlated system. Specifically, we demonstrate that ultracold dipolar fermions[30–32], e.g., ^{167}Er, ^{161}Dy, and ^{53}Cr, loaded in a two-leg ladder optical lattice serve as the first promising testbed of the reduction in one dimension, $\mathbb{Z} \to \mathbb{Z}_4$. Furthermore, we present a detailed account of how to experimentally access this phenomenon. In addition, we find intriguing gapless modes localized around the dislocations; even when the reduction occurs, gapless spin excitations are recovered around the dislocation which cannot emerge for non-interacting cases.

Reduction of topological classification in one-dimensional insulators, $\mathbb{Z} \to \mathbb{Z}_4$.- By employing a simple toy model, we first give an intuitive picture of the reduction in one dimension $\mathbb{Z} \to \mathbb{Z}_4$ in the presence of chiral symmetry arising from the structure of the bipartite lattice (for the definition, see Sec. I of supplemental material[33]). The corresponding symmetry class is AIII according to the Altland-Zirnbauer symmetry classes[34], indicating that the topology for non-interacting cases is characterized with the winding number. Recent studies based on the entanglement of the ground state[11] or field theories[24,28] revealed that the classification result is reduced from $\mathbb{Z}$ to $\mathbb{Z}_4$ due to correlations.

The reduction $\mathbb{Z} \to \mathbb{Z}_4$ can be observed by introducing interactions into the following two-leg Su-Schrieffer-Heeger (SSH) model composed of spin-half fermions,

$$H_0 = -\sum_{i\alpha}(V c^\dagger_{iA\alpha\sigma} c_{iB\alpha\sigma} + t c^\dagger_{i+1A\alpha\sigma} c_{iB\alpha\sigma}) + h.c., \quad (1)$$

where $c^\dagger_{is\alpha\sigma}$ creates a fermion in spin-state $\sigma(=\uparrow,\downarrow)$ at sublattice $s(=A,B)$ and chain $\alpha(=a,b)$ of site i. The lattice structure is shown in Fig. 1(a). Gapless edge modes of the above model are expected to be unstable against interactions. The reason is as follows[35]. Introducing the intra-chain Hubbard interactions would destroy the gapless charge excitations and would leave spin excitations gapless. Further introducing appropriate inter-chain interactions, e.g., spin exchange interactions, would gap out the remaining gapless edge modes. If the above argument indeed holds, it could verify the reduction $\mathbb{Z} \to \mathbb{Z}_4$[36].

Now the problems to be solved are as follows. (i) How can one implement the above model for the reduction $\mathbb{Z} \to \mathbb{Z}_4$ in cold atoms? (ii) How can one observe the reduction in experiments? Here, we naively think that introducing the kinetic spin exchange interaction of Heisenberg type between chains may be sufficient to realize the reduction. However, this scenario does not work because it breaks chiral symmetry[37] that is the key symmetry to be preserved in our study.

Dipolar fermions as a testbed of the reduction.- In the following, we propose how to prepare a promising and feasible platform for observing the reduction experimentally. Firstly, we note that the non-interacting part of the above model is considered to be feasibly prepared with optical lattices[38–42].

Now, we discuss how to prepare a system with chiral symmetry where fermions with (pseudo-)spin half interacts with each other by spin-exchange interactions. We find that this is accomplished by employing dipolar fermions (e.g., ^{167}Er, ^{161}Dy, and ^{53}Cr). Here, specifically, consider two ^{161}Dy atoms, labeled by 1 and 2. These atoms interact with each other via the magnetic dipole-dipole interaction[30]

$$U_{dd} = \frac{\mu_0(2\mu_B)^2}{4\pi r^3}[\boldsymbol{S}_1 \cdot \boldsymbol{S}_2 - \frac{3}{r^2}(\boldsymbol{S}_1 \cdot \boldsymbol{r})(\boldsymbol{S}_2 \cdot \boldsymbol{r})], \quad (2)$$

where $\boldsymbol{r} := \boldsymbol{r}_1 - \boldsymbol{r}_2$, and $\boldsymbol{r}_{1(2)}$ denotes the position vector of atom 1(2). $\boldsymbol{S}_{1(2)}$ denotes the total spin operator of electrons in the atom 1(2), respectively. μ_0 denotes the permeability of vacuum. μ_B denotes the Bohr magneton. Thus, loading ^{161}Dy atoms, one can prepare a system where fermions interact with each other via the magnetic dipole-dipole interactions. However, just loading the dipolar fermions is not sufficient, because ^{161}Dy atoms have huge spin $F = 21/2$, where F denotes the total spin of nuclear and electronic spins. Therefore, one has to restrict the Hilbert space spanned by the states with $m_F = 21/2, 19/2, \cdots, -21/2$ to the subspace spanned by two states, e.g. $m_F = 21/2, 19/2$, where m_F denotes the z-component of the spin.

The restriction of the Hilbert space is accomplished by the following three steps. (i) Prepare atoms in the states with $m_F = \pm 21/2, \pm 19/2$ by applying the optical pumping[43] which excites the states with $F = 21/2$ to the states with $F = 17/2$. (ii) Remove atoms in the states with $m_F = -21/2, -19/2$ by temporarily applying a magnetic field. (iii) Continue to shine the laser in the first step to forbid the transition via the dipolar relaxation[44] to the other states with $m_F = 17/2, 15/2, \cdots, -21/2$. The transition can be prevented due to the quantum Zeno effect[45]. We refer to the state with $m_F = 21/2$ ($m_F = 19/2$) as an effective up- (down-) spin state. Note that the intra-chain Hubbard interaction can be tuned by Feshbach resonance[46,47].

We thus end up with the following effective Hamiltonian:

$$\begin{aligned} H &= H_0 + U\sum_{i\alpha}(n_{is\alpha\uparrow} - \frac{1}{2})(n_{is\alpha\downarrow} - \frac{1}{2}) + J\sum_i h_{is}, \\ h_{is} &= A_1(\tilde{S}^x_{isa}\tilde{S}^x_{isb} + \tilde{S}^y_{isa}\tilde{S}^y_{isb}) - A_2\tilde{S}^z_{isa}\tilde{S}^z_{isb} \\ &\quad -A_3(n_{isa}-1)(n_{isb}-1) \\ &\quad -A_4[(n_{isa}-1)\tilde{S}^z_{isb} + (n_{isb}-1)\tilde{S}^z_{isa}], \end{aligned} \quad (3)$$

where $A_1 = 16^2/21$, $A_2 = 16/21$, $A_3 = 2 \times (160/21)^2$, $A_4 = (20 \times 16^2)/(21^2)$, respectively. [See Eq. (12) of supplemental material[33] for the explicit relation between U_{dd} and J.] Here, $\tilde{\boldsymbol{S}}$'s are pseudo-spin operators acting on the Hilbert space with $F = 21/2$ and $m_F = 21/2, 19/2$. We have assumed that the two chains are aligned along the z-direction, and that the distance between adjacent sites in the same chain is sufficiently large, allowing us to neglect the dipole-dipole interaction in the same chain[48]. The detail of the derivation is given in Sec. I of supplemental material[33]. Note that this system respects the chiral symmetry (see Sec. IB of supplemental material[33]). In experiments, the strength of the dipole-dipole interaction can be tuned by changing the distance between chains, l_0. The maximum strength is estimated to be $U_{dd} \lesssim 0.1t$ with $t \sim 1.0$kHz and $l_0 \sim 266$nm[48]. Thus, a realistic value of J in experiments is approximately $0 \lesssim J \lesssim 0.01t$.

Density-matrix renormalization group (DMRG) simulations for reduction: bulk and edge properties.- Now, using the DMRG method[49–51], we demonstrate that the reduction of topological classification occurs in our system. In the following, we restrict ourselves to the half-filled case. Let us start with the phase diagram of the intra-chain Hubbard interaction U vs. the inter-chain interaction J [Fig. 1(b)]. The phase diagram is obtained for $V = 0.1t$ under the open boundary condition (OBC). Unless otherwise noted, we set $V = 0.1t$ in the following. For small J, the system is in the chiral-symmetric phase while for large J, the system is in the charge-density-wave (CDW) phase, where the chiral symmetry is broken. We note that the CDW order breaks discrete symmetry and thus does not contradict the Mermin-Wagner theorem. The CDW order is induced by inter-chain density-density interaction in Eq. (3b).

Here, we note that under the periodic boundary con-

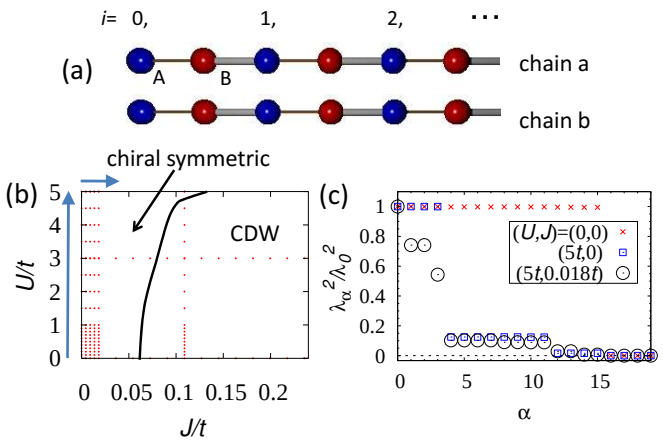

FIG. 1. (Color Online). (a): Sketch of the model (1). Blue (red) circles denote A (B) sublattice, respectively. Brown (gray) lines represent hopping V (t), respectively. (b): Phase diagram of the intra-ladder interaction U vs. the inter-ladder interaction J. Red dots are data points. (c): Highest 20 Schmidt eigenvalues (λ_α) for each case of parameters. Each eigenvalue is normalized with λ_0. These data are obtained under the OBC and for $L = 30$. For the calculation of the Schmidt eigenvalues (λ_α), we consider a virtual cut dividing the system at the strong bond (gray line) with $i = L/2$. We have observed the same structure of ES for larger L.

dition (PBC), the system is gapped for $0 \leq U \leq 5t$ with $J = 0$ and for $0 \leq J \leq 0.018t$ with $U = 5t$, respectively. These parameter regions are indicated as blue arrows in the phase diagram [see Fig. 1(b)]. Namely, the charge gap (Δ_c) and the spin gap (Δ_s) are open for these parameter sets, where the gaps are defined as $\Delta_c = E_{2L+1,1/2} - E_{2L,0}$ and $\Delta_s = E_{2L,1} - E_{2L,0}$ (L denotes the length of the chain), respectively. Here, $E_{N,\tilde{S}^z}$ denotes the lowest energy of the Hilbert space labeled by the total number of fermions and z-component of the total pseudo-spin. The charge gap and the spin gap are finite both in the chiral-symmetric phase and the CDW phase. For more detail of the bulk properties, see Sec. II of supplemental material[33].

The reduction occurs in the chiral-symmetric phase. Let us first observe the reduction via the degeneracy of the entanglement spectrum (ES) which is calculated in the bulk. Via the ES in the bulk one can deduce topological properties of the system; the degeneracy of the lowest entanglement energy states predicts the emergence of gapless modes around the edges[52]. In the following, we observe that the degeneracy of the ES is lifted as the interactions U and J are turned on. The 20 highest Schmidt eigenvalues, ${\lambda^2}_\alpha$, are plotted in Fig. 1(c) for several cases of parameters. The entanglement energy can be read off from the corresponding Schmidt eigenvalue via $E_\alpha = -2\log(\lambda_\alpha)$. For $(U, J) = (0, 0)$, the ES shows the 16-fold degeneracy in accordance with nontrivial topological properties of free fermions; the 16-fold degeneracy indicates gapless edge modes in the single-particle spectrum for each channel (α, σ), which is consistent with the winding number taking one for each channel (α, σ). Turning on the repulsive Hubbard interaction U lifts the degeneracy from 16-fold to 4-fold [see the data for $(U, J) = (5t, 0)$], indicating the emergence of gapless excitations only in a collective excitation spectrum. As we see below, these modes emerge in the spin excitation spectrum. Furthermore, turning on the inter-chain coupling J completely lifts the degeneracy of the ES; no degeneracy is observed for $(U, J) = (5t, 0.018t)$. Correspondingly, fermions in chain a and b form a singlet at each site. In the above, we have seen that introducing interactions, U and J, lifts the 16-fold degeneracy of the ES without chiral symmetry breaking. This result indicates the reduction of topological classification $\mathbb{Z} \to \mathbb{Z}_4$.

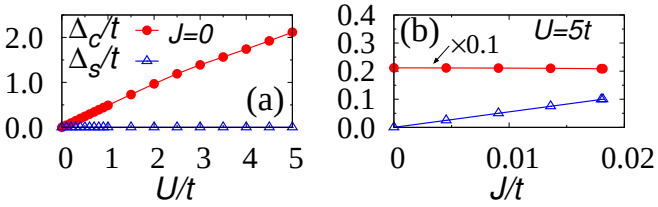

FIG. 2. (Color Online). (a) [(b)]: The charge gap Δ_c and the spin gap Δ_s as functions of the interaction strength under the OBC for $J = 0$ ($U = 5t$), respectively. In panel (b), the data of Δ_c is multiplied by 0.1.

Now let us turn to the edge properties. The presence/absence of gapless edge modes can be observed by comparing the results under the PBC and the OBC. In the following, we demonstrate that all of the edge modes for non-interacting systems are gapped out without symmetry breaking under the OBC. For $(U, J) = (0, 0)$, we can see that both of the charge and spin gaps are zero, indicating the emergence of gapless excitations around the boundary [Fig. 2(a)]. Switching on the interaction U opens the charge gap and keeps the spin gap zero, indicating the emergence of gapless edge modes only in the spin excitation spectrum [Fig. 2(a)]. Furthermore the introduction of J destroys the remaining gapless edge modes in the spin excitation spectrum [Fig. 2(b)].

Combining the result of the ES for the bulk and that of the excitation gaps for edges provides a comprehensive understanding of the reduction, $\mathbb{Z} \to \mathbb{Z}_4$. For more details, see Sec. II of supplemental material[33].

How to observe the reduction in experiments.- Our numerical simulation indicates that the opening of the charge and spin gaps at edges is a signal of the reduction. Now, the remaining problem we have to address is how to observe these excitation gaps.

To observe a gap opening of edge modes in the single-particle spectrum, we can make use of the local radio-frequency spectroscopy[53]. The gap size is estimated to be $\Delta_c \sim 2$kHz.

On the other hand, to detect the gap formation in spin excitations, a more elaborated method is necessary. We

find that it can be extracted from time-evolution of a superposed state composed of the ground state and the first excited state[54]. The basic idea is as follows[55]. Consider a wave function $|\psi(0)\rangle$ composed of a linear combination of the ground state $|1\rangle$ and an excited state $|2\rangle$, $|\psi(0)\rangle = c_1|1\rangle + c_2|2\rangle$ with $c_1, c_2 \in \mathbb{C}$. Under the time evolution, the state is written as $|\psi(t)\rangle = c_1 e^{-iE_1 t}|1\rangle + c_2 e^{-iE_2 t}|2\rangle$. Thus, the expectation value of an operator A is written as

$$\langle A(t)\rangle = \sum_i |c_i|^2 \langle i|A|i\rangle + 2a_{12}\cos[\omega_{21}t + \delta_{12}], \quad (4)$$

with $a_{12}e^{i\delta_{12}} := c_1^* c_2 \langle 1|A|2\rangle$, $a_{12} > 0$. By measuring the frequency, one can read off the size of the gap $\omega_{21} := E_2 - E_1$. Based on this prescription, one can observe the spin gap by (i) shining a half-π pulse only to the chain a and (ii) observing frequency of $\langle \tilde{S}^x_a(t)\rangle$ under the time-evolution with the Hamiltonian (3). Here, we explain the details of each step. First, shining the half-π pulse maps the singlet to the superposed state

$$\frac{1}{\sqrt{2}}|singlet\rangle + \frac{i}{2}[|\downarrow\rangle_a|\downarrow\rangle_b - |\uparrow\rangle_a|\uparrow\rangle_b], \quad (5)$$

where $|\sigma\rangle_{a(b)}$ with $\sigma = \uparrow, \downarrow$ describes the spins around the edges of chain a (b), respectively. $|singlet\rangle := (|\uparrow\rangle_a|\downarrow\rangle_b - |\downarrow\rangle_a|\uparrow\rangle_b)/\sqrt{2}$. The numerical results show that the energy of the triplet state with $\tilde{S}^z = 1$ and that with $\tilde{S}^z = -1$ is identical (see Sec. IV of supplemental material[33]). Second, in real experiments, $\langle \tilde{S}^x_a(t)\rangle$ can be measured by applying a half-π pulse (along $\tilde{S}^y$-axis) for both channels;

$$\langle\psi(t)|\Pi^\dagger_{1/2}\tilde{S}^z_a\Pi_{1/2}|\psi(t)\rangle = \langle\psi(t)|\tilde{S}^x_a|\psi(t)\rangle, \quad (6)$$

with $\Pi_{1/2} = \exp[i\pi(\sigma^x_a + \sigma^x_b)/4]$ arising from the half-π pulse. The matrices $\sigma_{a(b)}$'s denote the Pauli matrices acting on a fermion in pseudo-spin state of chain a (b), respectively.

The numerical simulation shows that the gap size is approximately $\Delta_s \simeq 0.1t \sim 100$Hz. Hence, at the lowest temperature achieved in two-component fermion systems, which is $T \simeq 0.25t$[56], thermal fluctuations significantly mix the singlet ground state with the excited states at edges. We can, however, prepare the singlet edge state by making use of feedback control[57,58] and a singlet-triplet oscillation[54] (see Sec. V of supplemental material[33]). In this way, by direct observation of excitation gaps under the OBC, we can access the reduction $\mathbb{Z} \to \mathbb{Z}_4$ in cold atoms.

Effects of dislocations on the reduction.- The high controllability of our system also allows us to study effects of dislocations, showing the following intriguing behaviors: even when the reduction occurs, gapless spin excitations are recovered around dislocations while single-particle excitations are gapped. To see this, let us consider a system with a dislocation described by L_d [Fig. 3(a)]. Fig. 3(b) indicates that the gap size of spin excitations decreases and finally becomes zero with increasing L_d, indicating the emergence of the gapless mode only in the spin excitations. This emergent gapless mode in the many-body spectrum is reminiscent of edge states emerging for the so-called topological Mott insulator[59–62] which can be understood in the following way: around the dislocation, the chain a does not couple with the chain b for $0 < i < L_d$, meaning that a single chain with the Hubbard interaction emerges for $i < L_d$. We consider that the above argument can be extended to higher dimensions.

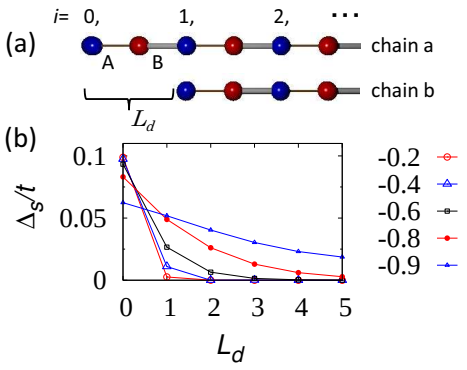

FIG. 3. (Color Online). (a): Sketch of a dislocation with $L_d = 1$. (b): The spin gap Δ_s for $V = 0.2t$, $0.4t$, $0.6t$, $0.8t$, and $0.9t$ in the presence of dislocations. The data is obtained for $(U, J) = (5t, 0.018t)$.

Conclusion.- Despite the rapid development of theory for the reduction of topological classification, an experimental observation is still missing and only very few setups have been proposed so far. In this paper, we have addressed this crucial issue and have proposed a promising experimental testbed for a realization of the reduction. The proposed setup with cold atoms allows us to turn on/off interactions in experiments, making distinct evidence available. The experimental platform can be implemented by loading ultracold dipolar fermions, e.g., ^{161}Dy atoms, into the two-leg SSH model and by making use of the quantum Zeno effect. We have also demonstrated how to observe the reduction experimentally, which can be feasibly done by direct measurements of energy gaps with the Radio frequency spectroscopy and the time evolution of superposed states. Furthermore, we have observed that even when the reduction occurs, gapless edge modes are recovered around the dislocations. Intriguingly, the edge mode localized around the boundary is distinct from the one for non-interacting cases. This edge state is reminiscent of a novel topological Mott insulator and can be another piece of solid evidence of the reduction. Our results are expected to impact on the correlated topological systems and are supposed to serve as a foothold for the experimental observation of the reduction in higher dimensions, and also for other novel correlated topological systems, such as

interaction enabled topological crystalline phases[63,64].

acknowledgements.- This work is partly supported by JSPS KAKENHI Grant No. 25220711, JP15H05855, and No. JP16K05501, and CREST, JST No. JPMJCR1673. The numerical calculations were performed on supercomputer at the ISSP in the University of Tokyo, and the SR16000 at YITP in Kyoto University.

[1] M. Z. Hasan and C. L. Kane, Rev. Mod. Phys. **82**, 3045 (2010).
[2] X.-L. Qi and S.-C. Zhang, Rev. Mod. Phys. **83**, 1057 (2011).
[3] A. Y. Kitaev, Physics-Uspekhi **44**, 131 (2001).
[4] J. Alicea, Reports on Progress in Physics **75**, 076501 (2012).
[5] M. Atala, M. Aidelsburger, J. T. Barreiro, D. Abanin, T. Kitagawa, E. Demler, and I. Bloch, Nature Physics **9**, 795 (2013).
[6] G. Jotzu, M. Messer, R. Desbuquois, M. Lebrat, T. Uehlinger, and D. Greif, Nature **483**, 302 (2012).
[7] S. Nakajima, T. Tomita, S. Taie, T. Ichinose, H. Ozawa, L. Wang, M. Troyer, and Y. Takahashi, Nature Physics **12**, 296 (2016).
[8] M. Lohse, C. Schweizer, O. Zilberberg, M. Aidelsburger, and I. Bloch, Nature Physics **12**, 350 (2016).
[9] B. Song, L. Zhang, C. He, T. F. J. Poon, E. Hajiyev, S. Zhang, X.-J. Liu, and G.-B. Jo, arXiv preprint arXiv:1706.00768 (2017).
[10] L. Fidkowski and A. Kitaev, Phys. Rev. B **81**, 134509 (2010).
[11] A. M. Turner, F. Pollmann, and E. Berg, Phys. Rev. B **83**, 075102 (2011).
[12] H. Yao and S. Ryu, Phys. Rev. B **88**, 064507 (2013).
[13] S. Ryu and S.-C. Zhang, Phys. Rev. B **85**, 245132 (2012).
[14] X.-L. Qi, New J. Phys. **15**, 065002 (2013).
[15] T. Neupert, L. Santos, S. Ryu, C. Chamon, and C. Mudry, Phys. Rev. B **84**, 165107 (2011).
[16] Y.-M. Lu and A. Vishwanath, Phys. Rev. B **86**, 125119 (2012).
[17] M. Levin and A. Stern, Phys. Rev. B **86**, 115131 (2012).
[18] L. Fidkowski, X. Chen, and A. Vishwanath, Phys. Rev. X **3**, 041016 (2013).
[19] Z.-C. Gu and X.-G. Wen, Phys. Rev. B **90**, 115141 (2014).
[20] C.-T. Hsieh, T. Morimoto, and S. Ryu, Phys. Rev. B **90**, 245111 (2014).
[21] C. Wang, A. C. Potter, and T. Senthil, Science **343**, 629 (2014).
[22] M. A. Metlitski, L. Fidkowski, X. Chen, and A. Vishwanath, arXiv:1406.3032 (2014).
[23] C. Wang and T. Senthil, Phys. Rev. B **89**, 195124 (2014).
[24] Y.-Z. You and C. Xu, Phys. Rev. B **90**, 245120 (2014).
[25] A. Kapustin, R. Thorngren, A. Turzillo, and Z. Wang, Journal of High Energy Physics **2015**, 1 (2015).
[26] H. Isobe and L. Fu, Phys. Rev. B **92**, 081304 (2015).
[27] T. Yoshida and A. Furusaki, Phys. Rev. B **92**, 085114 (2015).
[28] T. Morimoto, A. Furusaki, and C. Mudry, Phys. Rev. B **92**, 125104 (2015).
[29] T. Yoshida, A. Daido, Y. Yanase, and N. Kawakami, Phys. Rev. Lett. **118**, 147001 (2017).
[30] M. Lu, N. Q. Burdick, and B. L. Lev, Phys. Rev. Lett. **108**, 215301 (2012).
[31] K. Aikawa, A. Frisch, M. Mark, S. Baier, R. Grimm, and F. Ferlaino, Phys. Rev. Lett. **112**, 010404 (2014).
[32] B. Naylor, A. Reigue, E. Maréchal, O. Gorceix, B. Laburthe-Tolra, and L. Vernac, Phys. Rev. A **91**, 011603 (2015).
[33] Supplementary Material.
[34] S. Ryu, A. P. Schnyder, A. Furusaki, and A. W. W. Ludwig, New J. Phys. **12**, 065010 (2010) .
[35] T. Yoshida and N. Kawakami, Phys. Rev. B **95**, 045127 (2017).
[36] Destruction of all the edge modes in this model indicates that the two-leg SSH model (1) with the winding number four is topologically identical to the trivial phase.
[37] The kinetic spin exchange interaction ($\sim t'^2/U$) requires local interchain hopping t', which breaks the chiral symmetry.
[38] The SSH model for optical lattice has been already created[5,39]. The geometry of two-leg laddar can be created in experiments by means of the double-well optical lattice[39–42].
[39] S. Fölling, S. Trotzky, P. Cheinet, M. Feld, R. Saers, A. Widera, T. Müller, and I. Bloch, Nature **448**, 1029 (2007).
[40] J. Sebby-Strabley, M. Anderlini, P. S. Jessen, and J. V. Porto, Phys. Rev. A **73**, 033605 (2006).
[41] I. Danshita, J. E. Williams, C. A. R. Sá de Melo, and C. W. Clark, Phys. Rev. A **76**, 043606 (2007).
[42] Y.-A. Chen, S. D. Huber, S. Trotzky, I. Bloch, and E. Altman, Nature Physics **7**, 61 (2010).
[43] W. HAPPER, Rev. Mod. Phys. **44**, 169 (1972).
[44] S. Hensler, J. Werner, A. Griesmaier, P. Schmidt, A. Görlitz, T. Pfau, S. Giovanazzi, and K. Rzażewski, Applied Physics B **77**, 765 (2003).
[45] F. Schäfer, I. Herrera, S. Cherukattil, C. Lovecchio, F. S. Cataliotti, F. Caruso, and A. Smerzi, Nature communications **5** (2014).
[46] H. Feshbach, Annals of Physics **5**, 357 (1958).
[47] K. Baumann, N. Q. Burdick, M. Lu, and B. L. Lev, Phys. Rev. A **89**, 020701 (2014).
[48] S. Baier, M. J. Mark, D. Petter, K. Aikawa, L. Chomaz, Z. Cai, M. Baranov, P. Zoller, and F. Ferlaino, Science **352**, 201 (2016).
[49] S. R. White, Phys. Rev. Lett. **69**, 2863 (1992).
[50] U. Schollwöck, Rev. Mod. Phys. **77**, 259 (2005).
[51] U. Schollwöck, Annals of Physics **326**, 96 (2011), january 2011 Special Issue.
[52] H. Li and F. D. M. Haldane, Phys. Rev. Lett. **101**, 010504 (2008).
[53] T. Fukuhara, P. Schauß, M. Endres, S. Hild, M. Cheneau, I. Bloch, and C. Gross, Nature **502**, 76 (2013).
[54] D. Greif, T. Uehlinger, G. Jotzu, L. Tarruell, and T. Esslinger, Science (2013), 10.1126/science.1236362,.
[55] This argument is also applicable to measurement of the energy difference between the ground state and higher excited states (see Sec. III of supplemental material[33]).
[56] A. Mazurenko, C. S. Chiu, G. Ji, M. F. Parsons,

M. Kanász-Nagy, R. Schmidt, F. Grusdt, E. Demler, D. Greif, and M. Greiner, Nature **545**, 462 (2017).
[57] R. Inoue, S.-I.-R. Tanaka, R. Namiki, T. Sagawa, and Y. Takahashi, Phys. Rev. Lett. **110**, 163602 (2013).
[58] R. Yamamoto, J. Kobayashi, K. Kato, T. Kuno, Y. Sakura, and Y. Takahashi, Phys. Rev. A **96**, 033610 (2017).
[59] D. Pesin and L. Balents, Nat. Phys. **6**, 376 (2010).
[60] T. Yoshida, R. Peters, S. Fujimoto, and N. Kawakami, Phys. Rev. Lett. **112**, 196404 (2014).
[61] T. Yoshida and N. Kawakami, Phys. Rev. B **94**, 085149 (2016).
[62] X. Zhou, J.-S. Pan, Z.-X. Liu, W. Zhang, W. Yi, G. Chen, and S. Jia, Phys. Rev. Lett. **119**, 185701 (2017).
[63] M. F. Lapa, J. C. Y. Teo, and T. L. Hughes, Phys. Rev. B **93**, 115131 (2016).
[64] T. Yoshida *et al.,* in preparation.